Atmospheric Environment 166 (2017) 79–91

Contents lists available at ScienceDirect

Atmospheric Environment

journal homepage: www.elsevier.com/locate/atmosenv

Modeling study of biomass burning plumes and their impact on urban air quality; a case study of Santiago de Chile

G.C. Cuchiara [a, *], B. Rappenglück [a], M.A. Rubio [b, c], E. Lissi [b], E. Gramsch [d], R.D. Garreaud [e]

[a] University of Houston, Department of Earth and Atmospheric Science, Houston, TX, United States
[b] Facultad de Quimica y Biologia, Universidad Santiago de Chile, USACH, Av. L. B. O'Higgins 3363, Santiago, 9160000, Chile
[c] Centro Para el Desarrollo de la Nanociencia y Nanotecnología (CEDENNA-USACH), Santiago, 9160000, Chile
[d] Facultad de Ciencia, Depto Física, Universidad Santiago de Chile, USACH, Santiago, 9160000, Chile
[e] Center for Climate and Resilience Research, Department of Geophysics, Universidad de Chile, Santiago, 8320000, Chile

HIGHLIGHTS

- Unique case of biomass burning plume modeling in complex topography.
- Meteorological and air quality models provide insights about the transport of plumes and its chemical processing.
- Concentration, timing, and dispersion of the fire emissions were simulated.

ARTICLE INFO

Article history:
Received 21 January 2017
Received in revised form
1 June 2017
Accepted 4 July 2017
Available online 8 July 2017

Keywords:
Biomass burning
Atmospheric modeling
WRF/Chem
Plume rise model

ABSTRACT

On January 4, 2014, during the summer period in South America, an intense forest and dry pasture wildfire occurred nearby the city of Santiago de Chile. On that day the biomass-burning plume was transported by low-intensity winds towards the metropolitan area of Santiago and impacted the concentration of pollutants in this region. In this study, the Weather Research and Forecasting model coupled with Chemistry (WRF/Chem) is implemented to investigate the biomass-burning plume associated with these wildfires nearby Santiago, which impacted the ground-level ozone concentration and exacerbated Santiago's air quality. Meteorological variables simulated by WRF/Chem are compared against surface and radiosonde observations, and the results show that the model reproduces fairly well the observed wind speed, wind direction air temperature and relative humidity for the case studied. Based on an analysis of the transport of an inert tracer released over the locations, and at the time the wildfires were captured by the satellite-borne Moderate Resolution Imaging Spectroradiometer (MODIS), the model reproduced reasonably well the transport of biomass burning plume towards the city of Santiago de Chile within a time delay of two hours as observed in ceilometer data. A six day air quality simulation was performed: the first three days were used to validate the anthropogenic and biogenic emissions, and the last three days (during and after the wildfire event) to analyze the performance of WRF/Chem plume-rise model within FINNv1 fire emission estimations. The model presented a satisfactory performance on the first days of the simulation when contrasted against data from the well-established air quality network over the city of Santiago de Chile. These days represent the urban air quality base case for Santiago de Chile unimpacted by fire emissions. However, for the last three simulation days, which were impacted by the fire emissions, the statistical indices showed a decrease in the model performance. While the model showed a satisfactory evidence that wildfires plumes that originated in the vicinity of Santiago de Chile were transported towards the urban area and impacted the air quality, the model still underpredicted some pollutants substantially, likely due to misrepresentation of fire emission sources during those days. Potential uncertainties may include to the land use/land cover classifications and its characteristics, such as type and density of vegetation assigned to the region, where the fire spots are detected. The variability of the ecosystem type during the fire event might also play a role.

* Corresponding author. University of Houston, Department of Earth and Atmospheric Science, 4800 Calhoun Rd, Houston, TX, 77204-5007, United States.
E-mail address: gustavo.cuchiara@gmail.com (G.C. Cuchiara).

http://dx.doi.org/10.1016/j.atmosenv.2017.07.002
1352-2310/

1. Introduction

Wildfires are a significant direct source of atmospheric pollutants; on a global scale biomass burning is believed to be the largest source of primary fine particles in the atmosphere and the second largest source of trace gases after anthropogenic emission sources such as car emissions, agriculture and electricity generation (Crutzen and Andreae, 1990; Bond et al., 2004; Akagi et al., 2011, 2013). On a regional scale wildfires forest plumes are important due to the amount of primary pollutants such as carbon monoxide (CO), nitrogen oxides ($NOx = NO + NO_2$), and non-methane volatile organic compounds (VOCs), which can react with the sunlight and create hazardous secondary pollutants such as tropospheric ozone (O_3) (Morris et al., 2006; Real et al., 2007; Martins et al., 2012; Jaffe and Wigder, 2012).

The secondary pollutant O_3 is important for both health and climate implications (IPCC, 2007). Ozone is formed from the interaction of NO_x and VOCs in the presence of sunlight. The photochemistry relation NO_x-VOC-O_3 in urban environments have been studied for several decades and is reasonably well understood (Seinfeld and Pandis, 2016). Biomass burning plumes rich in O_3 and its precursors can be transported from the fire source area to nearby cities increasing the concentration of these pollutants and increasing the complexity of the atmospheric chemistry on urban areas. However, biomass burning can affect the tropospheric O_3 in different ways, depending on the distance of the fire source to the city. For instance, Cheng et al. (1998) reported an increase of O_3 production in Edmonton, Canada, located 300 km from the fire source area. On the other hand, for locations in Arizona, Texas, and western Mexico, Chalbot et al. (2013) reported a moderate decrease of O_3 in cities located less than 400 km from a fire source area. Another study performed during two fire periods in the greater Mexico City Metropolitan Area and its surrounding region in March 2006 did not show an evident difference in O_3 concentrations (Lei et al., 2013). However, the majority of studies suggest some degree of O_3 production from wildfires (e.g. Evans et al., 1974; Stith et al., 1981; Delany et al., 1985; Fishman et al., 1990; Kaufman et al., 1992; Thompson et al., 1996, 2001; Cheng et al., 1998; Fujiwara et al., 1999; Galanter et al., 2000; Kita et al., 2000; Forster et al., 2001; Jaffe et al., 2001, 2004; Liu et al., 2002; Yokelson et al., 2003, 2009; Colarco et al., 2004; Kondo et al., 2004; Bertschi and Jaffe, 2005; Junquera et al., 2005; Lapina et al., 2006; Morris et al., 2006; Pfister et al., 2006, 2008; Val Martín et al., 2006, 2008; Real et al., 2007; Oltmans et al., 2010).

The assessment of the impact of wildfires on air quality in cities is a complex task due to the superposition of biomass burning plumes of different chemical ages with the plethora of urban emission sources. Although the transport of O_3 and its precursors from one region to another is determined by flow patterns, i.e. the wind field, which can be obtained by measurements and/or modeling, the flow alone is insufficient in O_3 studies due to the complexity of chemistry involved. For this reason, many studies combine both measurements and modeling, to evaluate the impact of wildfire plumes over urban areas, and enhanced O_3 production due to mixing with urban NO_x emissions (e.g. McKeen et al., 2002; Junquera et al., 2005; Morris et al., 2006; Singh et al., 2010). A variety of models have been applied to study O_3 formation in wildfire plumes, e.g. MOZART-4, STEM, p-TOMCAT, CiTTyCAT, GEOS-CHEM, and GRACES (Pfister et al., 2008; Phadnis and Carmichael, 2000; Cook et al., 2007; Real et al., 2007; Nassar et al., 2009; Chatfield et al., 1996, respectively). Most of the models capture O_3 production, but fail to reproduce O_3 concentrations correctly (Jaffe and Wigder, 2012). Phadnis and Carmichael (2000) suggested that the model bias in the calculation of O_3 likely rises with uncertainties in the concentration, timing, and dispersion of the fire emissions. McKeen et al. (2002) observed biases in NO_x and VOC emission factors studying the long-range transport of plumes from Alaska and Canada. Simulations performed by Trentmann et al. (2003) revealed unrealistically low values of O_3 while simulating the first ten minutes of a fire plume. Mason et al. (2006) pointed out that an accurate VOC emission data is crucial to define the ability of the model to produce O_3 as the model reaction mechanism is very sensitive to changes in VOC emissions. Performing a box model simulation for a savannah fire plume Trentmann et al. (2005) found an underestimation up to 60 ppbv in O_3 production in the first hour of a plume. They attributed the low values to an incomplete understanding of the oxygenated VOC emission and photochemical reactions associated with these emissions. In a similar work using the GEOS-CHEM model, Alvarado et al. (2010) were capable of tracking biomass burning plumes over Canada, but the simulation showed that the boreal fires had a little impact on the median O_3 profile measured and within the smoke plumes observed by TES (Tropospheric Emission Spectrometer), probably due to the treatment of the VOCs in the model. Alvarado and Prinn (2009) simulated reasonably well the O_3 formation in African and Alaskan fire plumes using a Lagrangian parcel model, but reported an underestimation of the hydroxyl radical (OH) in their model simulation for Namibia. The authors reached this conclusion by raising OH in the model until O_3 matched with the observed values. In urban air quality simulation for the Houston area, Czader et al. (2013) found that OH underestimation was due to underestimations in ethene and formaldehyde, i.e. VOCs. which may also be crucial in fire emissions. In other words, the main lacunae preventing models to reproduce O_3 in biomass burning events properly are the misrepresentations of the O_3 precursors in the emission inventories within uncertainties generated by methods of calculations (e.g., plume representation in grid cells in Eulerian models).

Employing a high-resolution air-quality model (AQM) is essential to address air pollutant distribution, whenever local and regional transport of emissions occur. In three-dimensional models the representation of pollutant concentrations in a plume is also impacted by mixing and dilution which depend on the grid cell size imposing specific challenges for this particular simulation. In addition, many studies highlighted challenges to simulate O_3 in biomass burning plumes, that are associated with the accurate combination of a chemistry scheme with emission factors of the region modeled and the dynamics of the transported plume (Hauglustaine et al., 1999; Sinha et al., 2004; Pfister et al., 2006; Leung et al., 2007; Alvarado et al., 2010). Thus, the aim of this work was to perform an integrated approach combining measurements, fire emission inventory derived from satellite data, and temporal/spatial high-resolution modeling to examine a wildfire plume that impacted the air quality in Santiago, Chile, during the summer of 2014 (Rubio et al., 2015).

This paper is organized as follows. In the following section, we describe the Weather Research and Forecasting model coupled with Chemistry (WRF/Chem) model and its configurations used in this work (section 2.1). We also discuss some limitations and uncertainties related to fire emission inventory (section 2.2). In section 3 we give a brief description of the biomass-burning event with some characteristics of the area burned (section 3.1). After validating the meteorological variables against ground stations and radiosondes (section 3.2), a forward plume-rise simulation is described (section 3.3) releasing an inert tracer exactly where thermal anomalies were captured by satellite. This inert tracer simulation represents the transport of the biomass-burning plume by the mean wind. An analysis of WRF/Chem results to simulate surface ozone and its precursors in the metropolitan area of Santiago de Chile before and after the fire event is presented in section 3.4. Also in this section, a sensitivity analysis using fire emissions of

different emission strengths is performed and compared with the simulation without fire estimation. Finally, conclusions are compiled in the last section.

2. Methodology

2.1. WRF/Chem model and experimental design

This study consists of an experiment using the fully three-dimensional meteorology and chemistry WRF/Chem model applied to a wildfire event in the metropolitain area of Santiago de Chile during the southern hemispheric summer. The simulation is performed to recreate the biomass burning plume trajectory and analyze the impact of the fire emissions on the air quality in the city of Santiago, Chile.

The WRF model is used to provide a comprehensive analysis of the biomass burning event, combining both meteorological and chemical simulation and contrasting the results with observations. The WRF model was selected because it is a state-of-the-art three-dimensional weather prediction system designed to serve for both atmospheric research and operational forecasting needs (www.wrf-model.org). The WRF model is being used to study atmospheric dynamics and land-atmosphere interaction at various scales, ranging from few kilometers up to 1 000 km. The WRF physics options comprise several categories, each containing several choices. The physics categories include microphysics, cumulus parameterization, planetary boundary layer, land-surface model, and radiation. The chemistry package of WRF (WRF/Chem - Grell et al., 2005) is coupled to the dynamical and physical module of the meteorological model, and is responsible for simulating chemical processes such as gaseous and aqueous chemical reactions, dispersion, and deposition. The components of this modeling system, including chemistry and meteorology, employ the same transport, grid, boundary layer, and land surface model. The WRF/Chem setup for our experiment consists of the Noah land surface model (Tewari et al., 2004), the Lin's cloud scheme (Lin et al., 1983) the Grell-Freitas ensemble cumulus scheme (Grell and Freitas, 2014), the Yonsei University planetary boundary layer scheme (Hong et al., 2006), the RRTMG for short and long wave radiation scheme (Mlawer et al., 1997). The initial and boundary conditions for meteorological fields are provided by NCEP FNL data with a $1^\circ \times 1^\circ$ horizontal resolution.

The Regional Atmospheric Chemistry Mechanism (RACM) is the gas-phase chemical mechanism used in this simulation, which includes 237 reactions among 77 chemical species (Stockwell et al., 1997). The anthropogenic emissions used are obtained from REanalysis of the TROpospheric chemical composition (RETRO) modified with local sources according to Alonso et al. (2010). The Model of Emissions of Gases and Aerosols from Nature (MEGAN – Guenther et al., 2006) is applied to represent the net biogenic emissions. Every 6 h the Model for Ozone and Related Chemical Tracers version 4 (MOZART-4) provided updated initial and boundary condition for the chemical fields (Emmons et al., 2010). The Goddard Chemistry Aerosol Radiation and Transport (GOCART) model is used to simulate the major tropospheric aerosol components, including sulfate, dust, black carbon, organic carbon, and sea-salt aerosols. The PREP-CHEM-SRC (Freitas et al., 2011) is utilized as a pollutant emissions numerical tool to the spatial and temporal allocation of anthropogenic and aerosol emission sources in the model domain. The model results are output every hour, and the time step for the chemistry simulation is set to that used for the meteorological simulations, which is 40 s for the mother domain.

The Fire Inventory from NCAR version 1 (FINNv1) was implemented to provide daily varying emissions of trace species from biomass burning (Wiedinmyer et al., 2011). This method uses a combination of observations derived from the Moderate Resolution Imaging Spectroradiometer (MODIS) instrument aboard the NASA Terra and Aqua satellite, including rapid response fire detections, land cover type, and vegetation characteristics. The FINNv1 emissions database are released in the lowest model level, and WRF/Chem handles the plume-rise biomass burning pollutants.

We performed a simulation for the biomass burning case observed during January 2014 in Chile (Rubio et al., 2015) using three nested domains presented in Fig. 1a. The coarsest domain (Domain 1) has 36 km horizontal resolution and it covers part of the Chilean coast. The innermost nested domain (Domain 3) uses a grid spacing of 4 km and covers the metropolitan region of Santiago and the Melipilla region. The vertical configuration of the model comprises 42 layers, and the lowest 10 layers are below 2000 m a.g.l (above ground level). A set of four simulations were performed with the WRF/Chem model. The simulations have the same meteorological, chemical, physical and dynamical characteristics, the difference lies in the biomass-burning emissions as an input for the model. The simulations are initialized at 00 UTC, December 31, 2013, and the integration time is 7 days with the first 24 h considered spin-up time. Fig. 1b presents the satellite image showing the metropolitan area of Santiago, the Melipilla region, and the fire spots (red dots) detected by MODIS. The WRF/Chem simulation characteristics are compiled in Table 1.

In a first step, the WRF/Chem model results are contrasted against meteorological observations (air temperature, relative humidity, wind speed, and wind direction) from three ground stations inside the metropolitan area of Santiago, and the only radiosondes available during this period released from Santo Domingo (33.35° S, 72.63° W), which is located approximately 80 km west of Santiago's downtown. The Santo Domingo radiosondes are the nearest vertical profile available for Santiago's region. The three ground stations selected for this study present particular characteristics inside the urban area: the Cerrillos (CERR) station (33.49° S, 70.71° W, 528 m a.g.l), located on the west side of Santiago's downtown, is a low urban density station and considered an upwind location for this study; the Parque O'Higgins (POH) station (33.46° S, 70.66° W, 562 m a.g.l) in Santiago's downtown is located in a high urban density area; and the Las Condes (LC) station (33.37° S, 70.52° W, 811 m a.g.l), located at the northeast of Santiago's downtown, which is more complex location due to its proximity to the Andes and is considered an upwind site in this study. The chemical variables used to compare the WRF/chem model against observations are obtained from the same three ground stations. The chemical variables include ozone (O_3), carbon monoxide (CO), and nitrogen oxides ($NO_x = NO + NO_2$). These data sets provide a unique case to assess the performance of biomass burning plume modeling in complex topography and validated by an established air quality network. The complexity of the terrain is due to the location of Santiago de Chile basin in the immediate vicinity of the highest mountain ranges of the Andes to the east and the Cordillera de la Costa to the west, with terrain heights ranging from about 500 m agl to 6 km a.g.l (see Fig. S1 in the Supplementary Material for the terrain height on grid d03). More information regarding the meteorological and chemical observations is provided in Rubio et al. (2015).

Comprehensive statistical analysis is performed to evaluate the relationship between O_3, NO_x, and CO, simulated by WRF/Chem vs. observations. The calculated parameters include the coefficient of determination (R) to determine the strength of linear association between forecasts and observations, the root mean square error (RMSE), to describe the magnitude of the difference between predicted and observed values, and the bias (BIAS) to define the expected error due to the model mismatch. The statistical analysis for the chemical variables are applied for three different periods: the

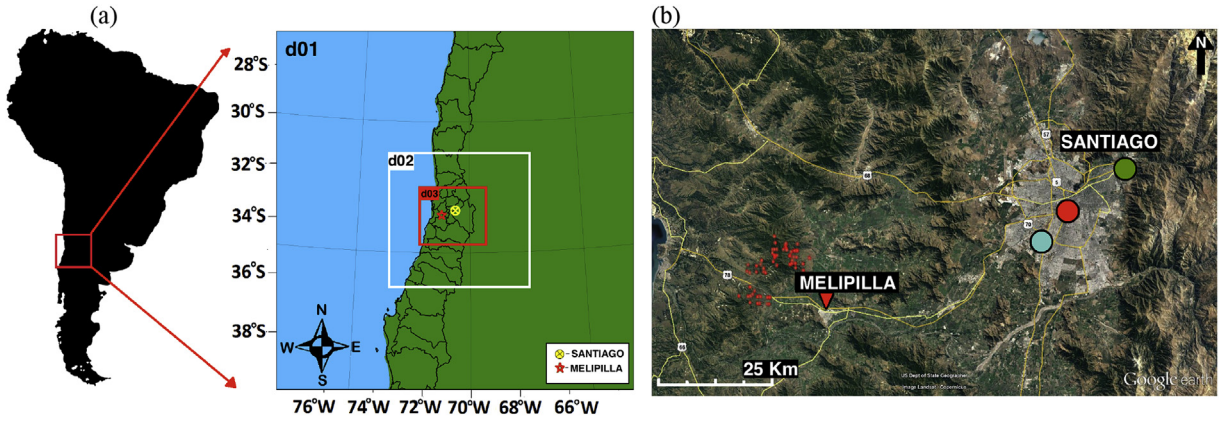

Fig. 1. WRF/Chem domain configuration (a) and satellite image of Santiago region (b) with the location of fires detected by MODIS (red dots) and the urban stations CERR (blue circle), POH (red circle), and LC (green circle). (For interpretation of the references to colour in this figure legend, the reader is referred to the web version of this article.)

Table 1
Parameters in the WRF/Chem simulation.

Domain	1	2	3
Period		December 31, 2013, to January 06, 2014	
Initial condition meteorology		NCEP FNL (1° × 1° horizontal resolution)	
Initial condition chemistry		MOZART-4 (2.8° × 2.8°)	
Horizontal grid (x,y,z)	135 × 135	125 × 125	151 × 136
Horizontal resolution	36 km	12 km	4 km
Time step	40 s	10 s	4 s
Microphysics		Lin	
Long and short wave radiation		RRTMG	
Land surface		Noah	
Planetary boundary layer		YSU	
Chemistry mechanism		RACM	
Anthropogenic emission		RETRO	
Biogenic emission		MEGAN	
Fire emission		FINNv1	
Aerosol emission		GOCART	
Dry deposition		Wesley	
Photolysis		Madronich TUV	

total simulation period (144 h); the period before the day the biomass-burning plume is observed in the metropolitan region of Santiago (January 1 to 3, 2014; 72 h); and the period when the biomass-burning plume impacts metropolitan region of Santiago (January 4 to 6, 2014; 72 h).

2.2. Limitations, uncertainties and model experiments

Although the fire emission inventory (FINNv1) is useful for multiple applications, because it produces spatially and temporally high-resolution (daily; gridded ~1 km^2) emission from open biomass burning on a global scale, the estimates are very uncertain and have just begun to be compared to observations and other biomass burning inventories (Pfister et al., 2011; Wiedinmyer et al., 2011). Many uncertainties regarding the estimations are described in detail by Wiedinmyer et al. (2006, 2011) and will be briefly discussed in this work. Uncertainty could arise due to relative small fires resulting in an underestimation of the number of fires, misidentification of the land cover, inaccurate fuel loading and parameterizations of combustion completeness, and both uncertainty and natural variation in the emission factor (Wiedinmyer et al., 2011; Akagi et al., 2011). Also, as our work includes hourly simulation, another uncertainty arises from the temporal resolution of the MODIS dataset, which is provided on a daily basis. Satellite overpass timing and cloud cover may prevent the detection of different stages of fire emission.

MODIS detects fires in 1 km pixels that are burning at the time of overpass under relatively cloud-free conditions using a contextual algorithm, and the location and timing for the fires are identified globally by the Thermal Anomalies Product (Giglio et al., 2006). In our study the MODIS overpass on day Jan 04 captured 56 hotspots (Supplementary Material Fig. S2) and those fires were allocated in 15 grid cells (GC). Fig. 2 shows the position of these 15 GC representing the mean fire size (km^2) in the domain d03. Table 2 shows the values of mean fire size in Fig. 2 for each GC, and the fraction of each land use classifications (Savanna (SV), Extratropical Forest (EF) Tropical Forest (TF), and Grassland (GR)) of the total fire size in the GC. Note that the GCs are numbered starting from the upper left GC. The mean fire size calculated by the model was 10.33 km^2, which represents 5 km^2 less than the observed size. This is because at present, FINNv1 does not obtain the area burned at each identified fire pixel from burned area products, since they are not rapidly available. Therefore, an upper limit of 1 km^2, is assumed except for fires located in grasslands/savannas, which are assumed 0.75 km^2 for the burned area. (Wiedinmyer et al., 2011). Note: based on the fraction of each classification (Table S1 in the Supplementary Material) the predominant vegetation was savanna.

The emission estimations for CO, NO_x, and non-methane organic compounds NMOC for every hour of Jan 4 are presented in Fig. 3 and the values of each GC are given in Table 2. The total amount of emissions was 5 333.98 mol $km^{-2}hr^{-1}$, 152.50 mol $km^{-2}hr^{-1}$, and 718.60 mol $km^{-2}hr^{-1}$ for CO, NO_x, and NMOC, respectively. The

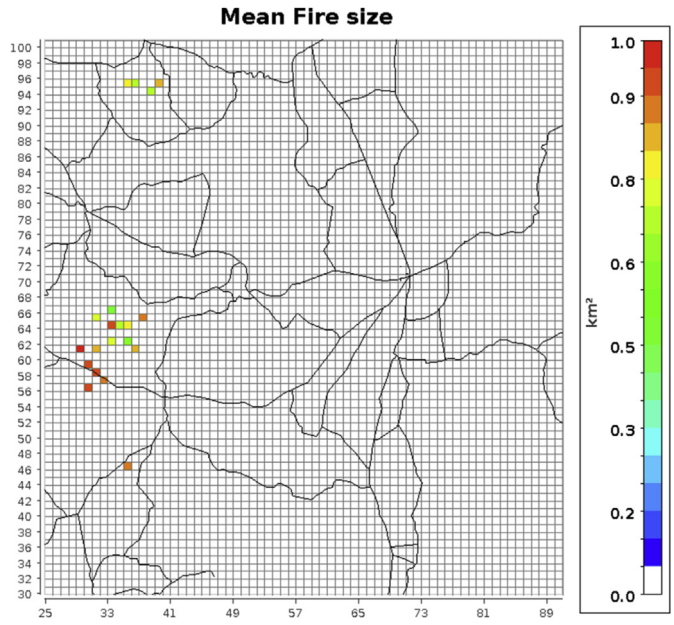

Fig. 2. Mean fire size (km^2) in the grid d03.

model injection height is estimated to be between 1.8 and 2 km agl, which agrees with 6000 ft agl reported from news coverage in the Chilean media based on visual observations aboard aircrafts during the event (Gallardo, 2014).

The original idea in this work was to use another source of fire emissions such as the Global Fire Emission Database, version 4 (GFED4 – Randerson et al., 2015) to be compared with FINNv1. However, we faced some limitations: 1) the horizontal resolution of the dataset (0.25 × 0.25-degree), which is relatively coarse for the simulation resolution proposed in our case (5 km resolution), making it difficult to compare it with the fire characteristics calculated by FINNv1; 2) currently, the preprocessor of emissions in the WRF/Chem (PREP_CHEM_SRC - Freitas et al., 2011) generates fire emission using the version 2 of GFED, which covers only the years from 1997 to 2008. These limitations discouraged us to perform a simulation with this dataset, but we provide at least some emissions estimates from GFED4 raw data for comparison with FINNv1 data. Following the information and calculation results given in Table S2 in the Supplementary Material the estimated ratio of FINNv1 to GFED4 emissions for NO_x, NMHC, and CO, are approximately 10, 1.6, and 0.15, respectively. Thus, the FINNv1 shows higher emissions for NOx and NMHC, and lower emissions of a factor of 6 for CO.

As stated by Reid et al. (2009), current regional emission estimates still have integer factors of uncertainty. In addition, the authors mentioned that MODIS land cover resulted in regionally variable difference of a factor of 2 or more in emissions. For this reason and the amount of uncertainty, we performed an extra set of four WRF/Chem simulations in contrast to just one base simulation, which does not have emissions from fire (NOFIRE); one simulation with the standard emission calculated by FINNv1 (FIRE); and three extra simulations taking into consideration possible underestimation of fire emissions related to the uncertainties described above. For this exercise, we performed simulations with four (FIRE_4X), and an extreme case of eight (FIRE_8X) times the standard fire emission.

3. Results and discussion

3.1. The biomass-burning event

During January 2014, in the southern hemispheric summer, strong wildfires in forest and dry pastures took place in the Melipilla region (Fig. 1b), which is located approximately 70 km southwest of the metropolitan area of Santiago. The area burned by the fire comprised approximately 15 km^2, and the land coverage were characterized by a mixture of pasture, open woodland and shrubland, including *Eucalyptus* and *Acacia caven trees* (Armesto et al., 2007; Schulz et al., 2010; Rubio et al., 2015). Particularly on January 4, SW low-level winds at 2-3 ms^{-1} (Rubio et al., 2015) were favorable for the transport of plumes originated from the wildfire towards Santiago downtown as shown in satellite images (Fig. 4). Fig. 4a and b shows the corrected reflectance (true color) images from MODIS for January 4, 2014.

3.2. Meteorology simulation

Fig. 5 presents the comparison of surface wind speed and direction between observation and the WRF model results for the simulation period. The time-period comprising the comparisons covers 6 days, including the biomass-burning episode days in Santiago de Chile. The model appropriately reproduced the diurnal variation with a slight overestimate (approximately 2–4 m/s) of the wind speed during daytime at POH and LC (Fig. 5b and c, respectively). Despite the complex topography of Santiago de Chile, the model simulated reasonably well the wind direction at all stations, capturing the diurnal shifts of the wind direction. Synoptic (day-to-day) variability was small during this summer period. Comparisons for air temperature and relative humidity can be found in Fig. S3 in the Supplementary Material.

The analysis made for the ground stations was extended to vertical profiles using radiosonde launches from Santo Domingo, the only available radiosonde facility in the Santiago region. As a

Table 2
Statistical analysis for simulation without fire emission estimations.

	O_3			NO_x			CO		
	LC	POH	CER	LC	POH	CER	LC	POH	CER
R (1–3)	0.89	0.92	0.90	0.53	0.70	0.67	0.32	0.47	0.56
R (4–6)	0.87	0.80	0.74	0.13	0.87	0.73	−0.17	0.17	−0.01
R (Total)	0.81	0.82	0.78	0.45	0.80	0.70	0.07	0.22	0.16
RMSE (1–3) ppb	13.04	8.33	9.51	10.44	8.69	9.75	150.55	611.18	98.51
RMSE (4–6) ppb	45.33	27.19	27.00	12.70	15.82	22.93	527.24	458.16	610.53
RMSE (Total) ppb	25.61	20.17	20.30	11.06	12.79	17.66	388.85	539.59	438.72
BIAS (1–3) ppb	9.35	5.30	6.68	−1.24	−1.17	−0.39	42.08	569.79	42.76
BIAS (4–6) ppb	11.64	15.58	15.89	1.47	7.44	10.55	381.90	342.58	442.20
BIAS (Total) ppb	10.42	10.37	11.20	0.11	3.11	5.05	210.53	453.04	240.81

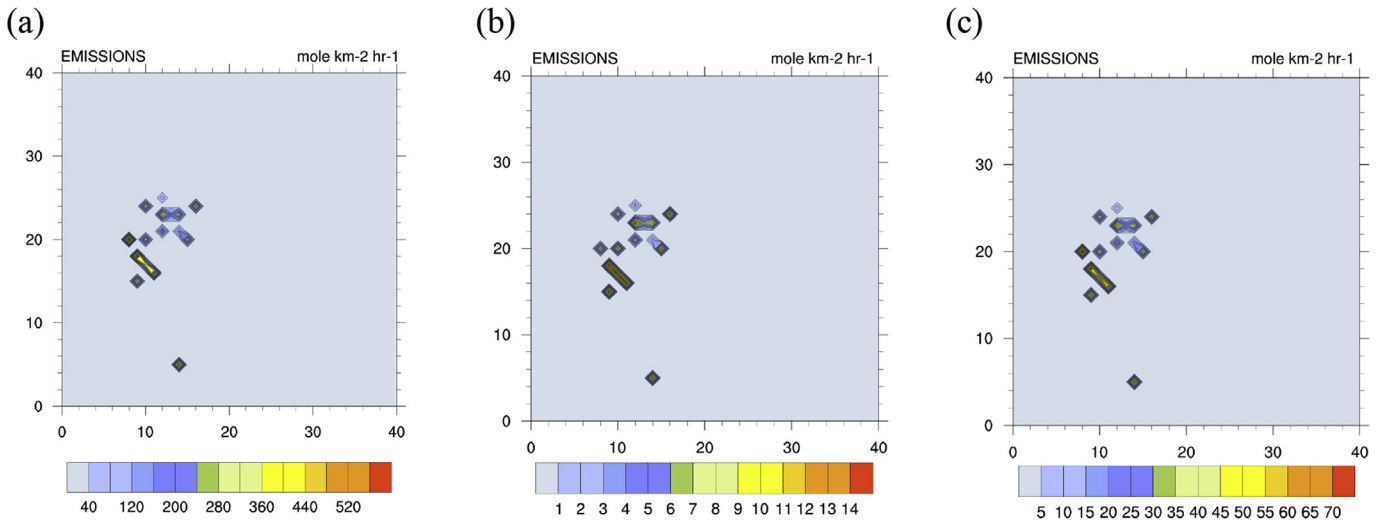

Fig. 3. Emissions of CO (a), NO_x (b), and NMOC (c) in mole $km^{-2}hr^{-1}$ for the region where active fires were captured.

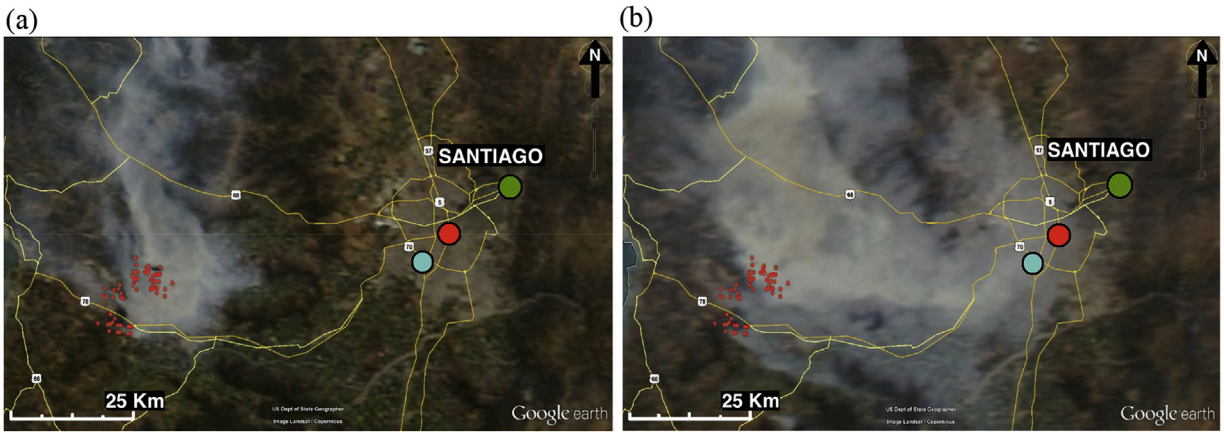

Fig. 4. Corrected reflectance Aqua satellite image captured over Santiago at approximately 11:00 LT (Fig. 4a) and the satellite Terra image obtained at approximately 15:00 LT (Fig. 4b) on January 4, 2014.

typical result Fig. 6 shows the comparison between observed and simulated air temperature (a), relative humidity (b), wind speed (c), and wind direction (d) for January 04 at 12:00 UTC (09:00 LT). The simulated air temperature and relative humidity comparisons (a and b) present a fairly good agreement with the observations, capturing the inversion layer between 500 and 1 000 m a. g. l. Also, the comparison with wind speed and direction (c and d, respectively) show a reasonably good agreement with radiosonde measurements. Up to an altitude of approximately 800 m a.g.l. the model overestimates the wind speed up to 5 m/s. This bias was likely downscaled from meteorological NCEP/FNL input data. The reasonably good performance of the meteorology simulation provides confidence for the next steps of this study, the plume transport analysis, and the chemistry simulation.

3.3. Forward plume-rise transport

Fig. 7 presents the forward plume-rise transport of an inert tracer calculated by WRF/Chem for the period between the two satellite images from 11:00 to 15:00 LT on January 04, 2014 (see Fig. 4a and b). The modeled inert tracer represents the temporal and spatial distribution of biomass burning plume starting at the location where the fire was captured by MODIS on satellite Aqua/Terra (Fig. 4a and b) throughout thermal anomalies of temperature. Fig. 7a presents the simulated inert tracer at 11:00 LT, which correspond to the approximate time of the satellite image (Fig. 4a). Visually comparing the simulated and observed plume as seen in the satellite images it is possible to identify some similarities in the shape and position of the plume. In this case the biomass-burning plume is being transported northward downwind of the Melipilla region not impacting the metropolitan region of Santiago. The next steps of the simulation show the times 12:00, 13:00, and 14:00 LT (Fig. 7b, c, and 7d). During these times the simulated biomass-burning plume shifts its transport direction due to the shift of wind direction (Fig. 5d, e, and f) from south to southwest, transporting the plume towards Santiago. This shift of the wind direction is reported by Rutllant and Garreaud (2004; their Fig. 5c) as a typical pattern of the local circulation that develops during the afternoon during summer months. Also, as stated by Rubio et al. (2015) the biomass-burning plume that originated during the morning hours took less than 3 h to reach the city of Santiago. The plume was observed at 14:00 LT through a sharp increase in the reflectivity captured in the ceilometer data (see Rubio et al., 2015, their Fig. 4). Although the inert tracer representing the biomass-burning plume was reasonably well simulated by WRF/Chem, the simulated plume has an arrival delay of two hours in the city of

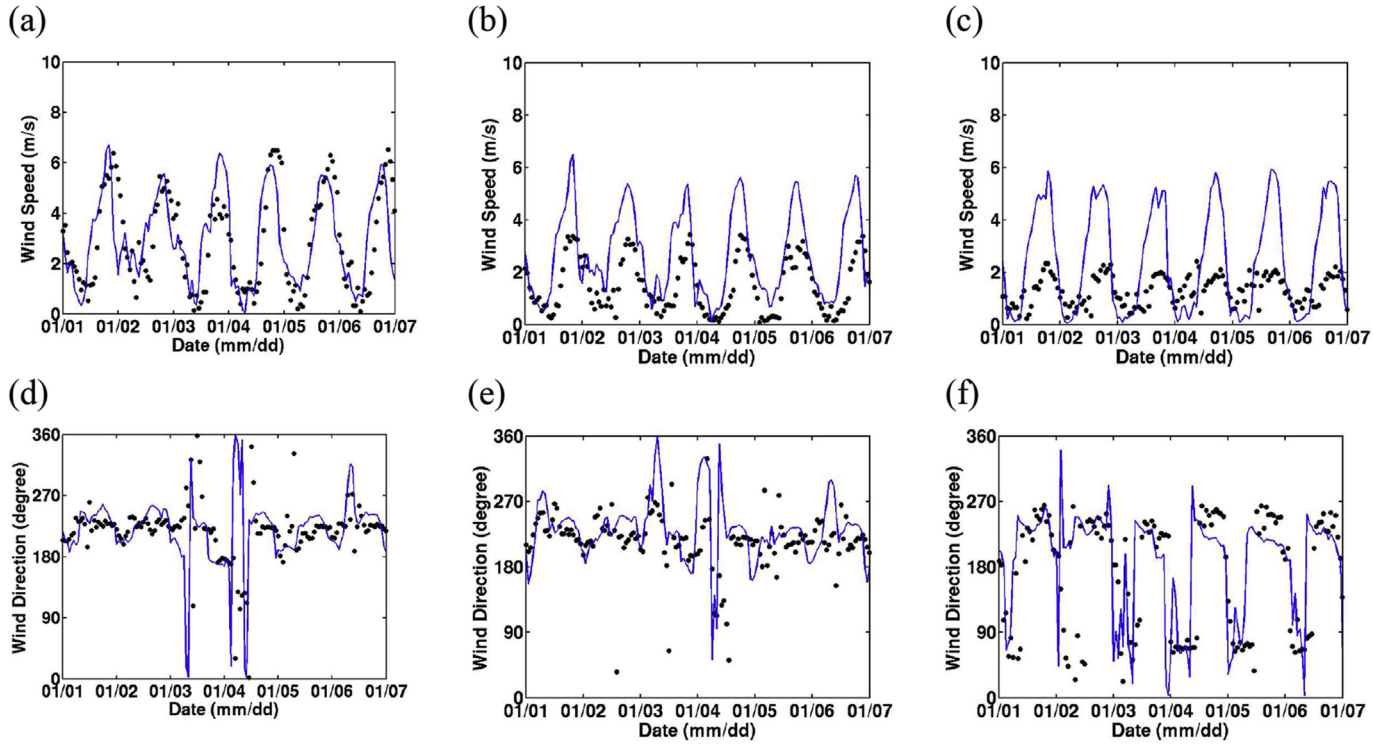

Fig. 5. Observed (dots) versus modeled (line) time series of wind speed (a, b, and c) and wind direction (d, e, and f) for urban stations CERR (first column), POH (second column), and LC (third column) for January 01–07, 2014.

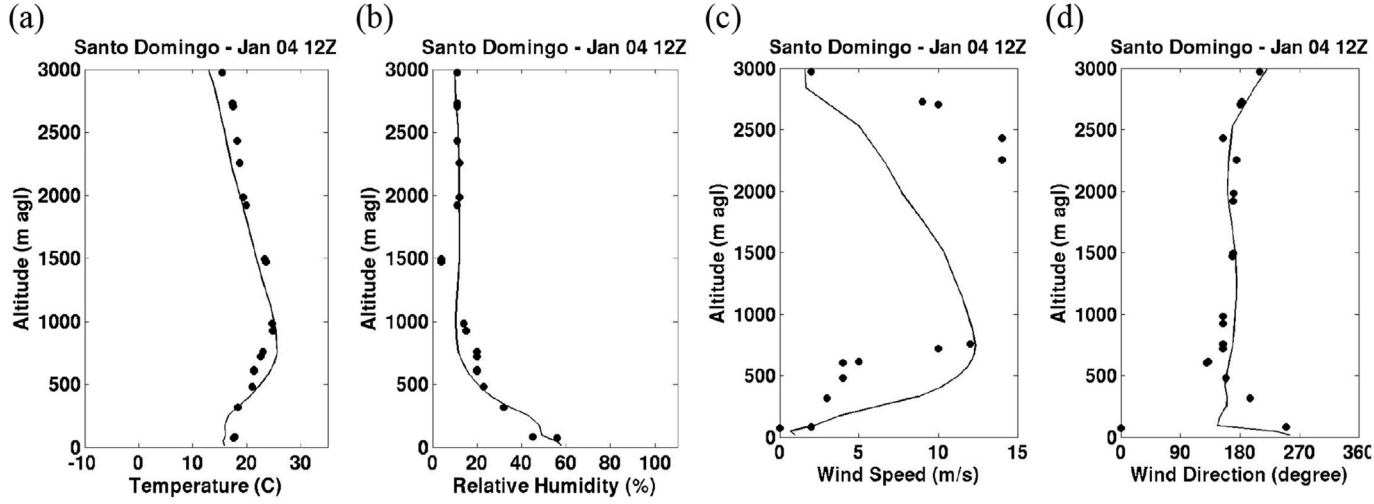

Fig. 6. Simulated vertical profiles of air temperature (a), relative humidity (b), wind speed (c), and wind direction (d) as calculated by WRF/Chem at 9:00 LT on January 04, 2014.

Santiago. The delay in the arrival of the plume can result in a misrepresentation of pollutants inside the plume arriving at the city of Santiago due to photochemical aging, and likely has an important impact on the simulation of O_3 mixing ratios.

3.4. Chemistry simulation

After ensuring that the simulation reasonably represented the transport of the biomass-burning plume toward the city of Santiago, a more detailed assessment of the air quality impacts of the fires was performed using WRF/Chem. In this analysis, a set of four WRF/Chem simulations were performed: the first without fire emissions, the second with fire emission estimated by FINNv1, and two extra simulations with four and eight times the amount of emission estimated by FINNv1. The difference between these simulations helps us to characterize the impact of the fires magnitude.

For the first task, i.e., the simulation without fire emission sources, the goal was to perform a model validation for the O_3 and its precursors NO_x and CO, especially for the period between January 1 at 00 LT to January 4 at 00:00 LT (before the fire). This exercise can guarantee that the emissions over Santiago are sufficiently well represented by the global emission inventories (RETRO with adjustments made by Alonso et al., 2010, and MEGAN) during days without the impact of fire emissions. To our knowledge this

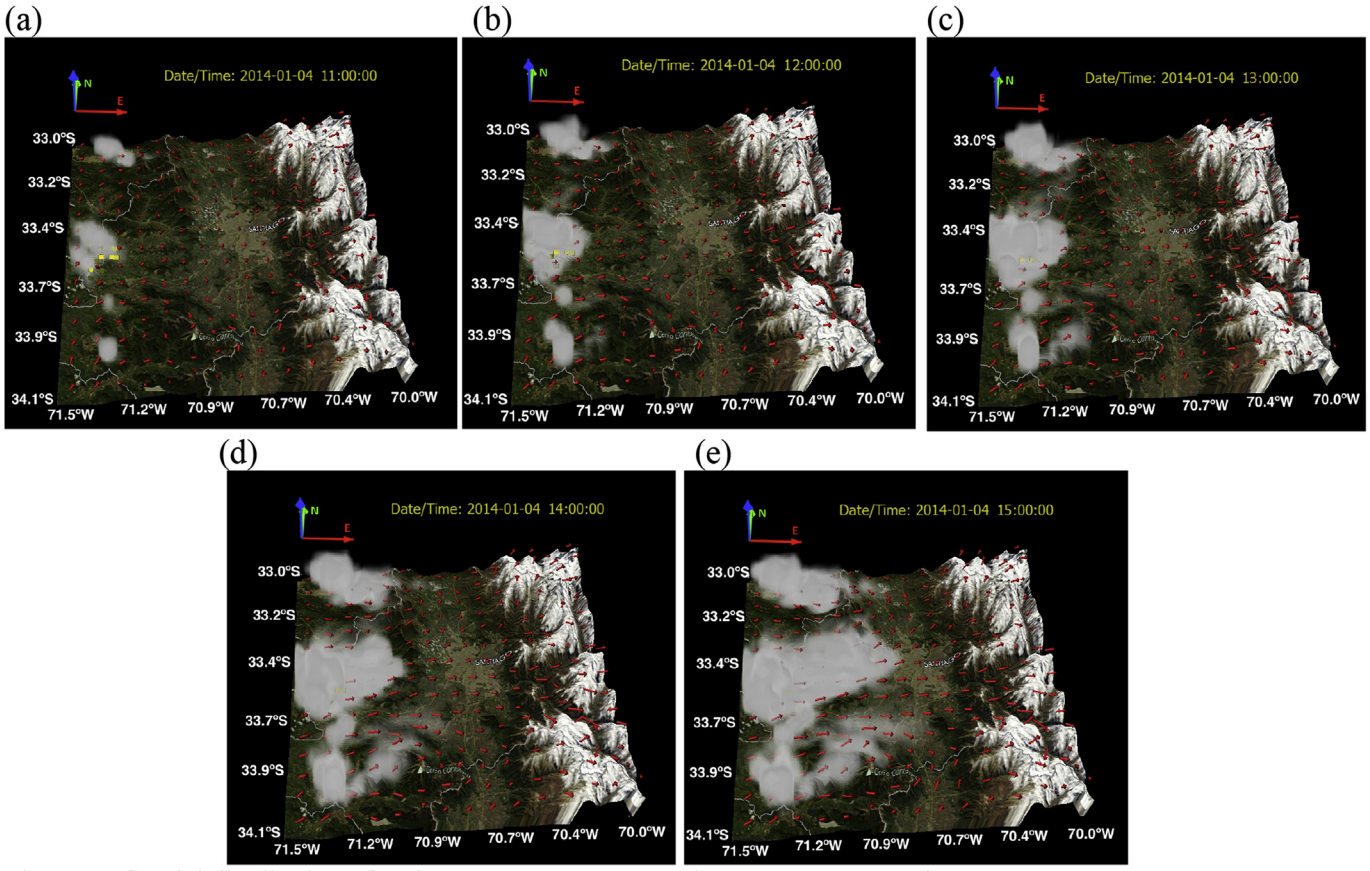

Fig. 7. Spatial distribution of an inert tracer at (a) 11:00 (b) 12:00 (c) 13:00 (d) 14:00 (e) 15:00 LT on January 4, 2014 (www.vapor.ucar.edu).

work is the first study that attempts to validate a regional air quality simulation over the city of Santiago using this set of emission inventories. Ozone time series, and their respective scatter plot are presented in Fig. 8 for the three stations (CERR, POH, and LC, respectively) from January 1 to 6, 2014. The scatter plots are divided into three different periods: (i) before the fire event from January 1 to 3 (circles), (ii) during the fire event January 4 (cross), and (iii) after the fire event on January 5 and 6 (triangles). The same analysis was made for NO_x and CO (see Fig. S4 in the Supplemental Material). As shown in Fig. 6 the model shows a good agreement with the O_3 mixing ratios observed before the plume reaches the city of Santiago. Although the diurnal variation of O_3 is being well represented by the model at the LC station (Fig. 8c) the minimum values during the night and the maximum values during daytime were underestimated. The LC station is a very complex location to be modeled since it is located right at the foothills of the Andes in a very complex terrain. The complexity in the topography can result in local circulations not captured by the model horizontal resolution. The overestimation of wind speed (Fig. 5a) in this station is likely limiting the representation of pollutant concentration at this grid point, consequently transporting pollutants away. This can limit both the formation of O_3 during daytime and the titration of O_3 during nighttime. After 14:00 LT on each day the model tends to strongly underestimate the O_3 mixing ratios (up to 100 ppb of O_3 during the fire event) for all the stations. This underestimation can be due to an emission source not represented in the simulation such as fire emission. The statistical analysis of the simulation results versus observed data for O_3, NO_x, and CO are presented in Table 2, and reinforces what is displayed in Fig. 8 and Fig. S4. During the first three days (1–3) of simulation (i.e. without biomass burning emissions reaching the city of Santiago) ozone shows high R values (0.89, 0.92, and 0.90) and lower RMSE (13.04, 8.33, and 9.51 ppb) and BIAS (9.35, 5.30, and 6.68 ppb) values for LC, POH, and CERR, respectively. On the other hand, during and after the fire event (4–6) the chemistry in the Santiago air shed is likely impacted by biomass burning emission which is reflected by a reduction in statistical indices values of R (0.87, 0.80, and 0.74), RMSE (45.33, 27.19, and 27 ppb), and BIAS (11.64, 15.58, and 15.89 ppb). The same results can be found made for CO and NO_x, except for POH and CERR stations, where R index shows higher values in the January 4 to 6 period compared with the January 1 to 3 period.

A key finding in Rubio et al. (2015) was the enhanced ozone mixing ratios enhanced during the wildfire events observed in all stations in the Santiago basin. Fig. 9 presents a sensitivity study of the O_3 mixing ratios simulated with the different fire emission strengths impacting the study area. These simulations are termed as NOFIRE (blue), FIRE (yellow), FIRE_4X (green), and FIRE_8X (red), and compared against observed values for the three stations LC, POH, and CERR on January 04. The two extra runs (FIRE_4X and FIRE_8X) were important to assess possible uncertainties of FINNv1 estimations (see section 2) due to the high complexity of emissions in wildfires events. Based on the results it is possible to infer that the magnitude of the fire emissions by FINNv1 is likely underestimated for this case; therefore, O_3 mixing ratios only show a slight increase of up to few parts per billion. On the other hand, the bigger the increase in the magnitude of the biomass-burning emissions are the more evident were the impact of the emissions in the formation of O_3, and the impact on O_3 was up to 10–15 ppb for FIRE_4X and up to 20–25 ppb for FIRE_8X. The results show that

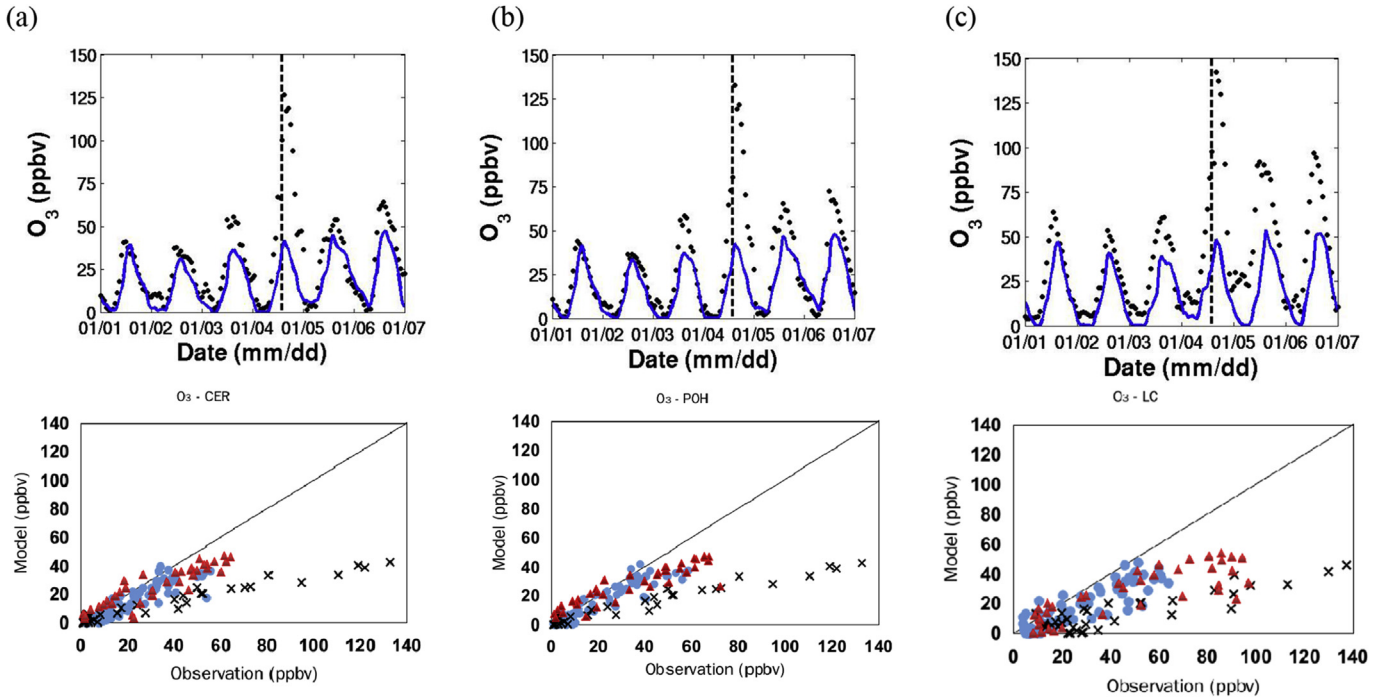

Fig. 8. Time series of observed and simulated O_3 mixing ratios and their respective scatter plot for CERR (a), POH (b), LC (c), for January 1–6, 2014. The dashed line represents the time where the biomass burning plume was observed in the ceilometer data (14:00 LT).

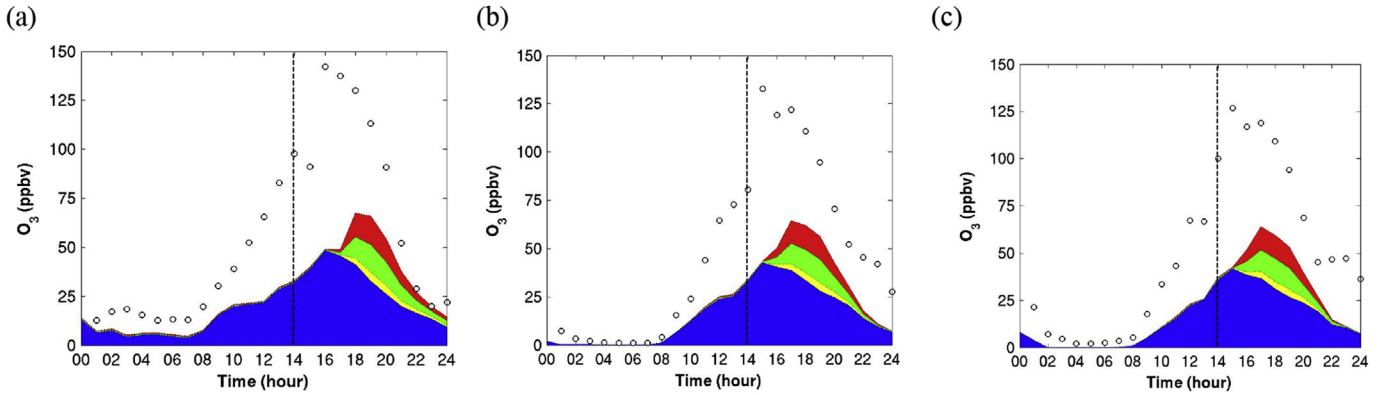

Fig. 9. Time series of the observed and simulated O_3 mixing ratios for the NOFIRE (blue), FIRE (yellow), FIRE_4X (green), and FIRE_8X (red) for CERR (a), POH (b), LC (c), for January 4, 2014. (For interpretation of the references to colour in this figure legend, the reader is referred to the web version of this article.)

the wildfire emissions reached Santiago and impacted the air quality in the city as stated by Rubio et al. (2015). While the combination of WRF/Chem and FINNv1 estimates present an excellent tool to investigate fire events on a regional scale there remain some uncertainties (e.g. underestimation of small fires, misidentification of the land cover, natural variation of emission factors, etc.) that need to be further investigated.

In a final O_3 analysis, we examined the impact of the highest magnitude of fire emissions (FIRE_8X) on O_3 mixing ratios. Fig. 10 presents the spatial distribution of ΔO_3, i.e. the difference between O_3 mixing ratios simulated without fire emission and the highest factor applied to FINNv1 estimations (FIRE_8X), in the domain d03 for 18 LT (time of the highest O_3 mixing ratios calculated by WRF/chem) on January 04, 2014. ΔO_3 mixing ratios at the three ground sites were approximately 28, 32, and 36 ppb, respectively, at this hour of the day. However, as mentioned earlier the 2-h delay of the plume arrival in Santiago could result in an underestimation of the highest O_3 mixing ratios not only due to the complex and often pronounced diurnal variation of the main O_3 precursors in Santiago de Chile (Rappenglück et al., 2000, 2005; Elshorbany et al., 2009) besides, high O_3 values would require a combination of high O_3 precursors concentrated in the same region and during the peak radiation of the day. Thus, not only the time of the plume arrival mentioned before, but also the shape of the plume and its transport over very complex terrain can lead to O_3 misprediction. Fig. 10 shows ΔO_3 values up to 40 ppb calculated by WRF/Chem. These results do not necessarily coincide with the grid point analysis shown in Fig. 8.

During the wildfire event ozone mixing ratios exceeded 80 ppb at all three stations which is relatively high compared to background values. Rubio et al. (2015) stated that relatively high NO_2/NO_x emissions in biomass burning would lead to high O_3 mixing ratios almost independently of precursor emissions, as such high NO_2/NO ratios would not need to be generated

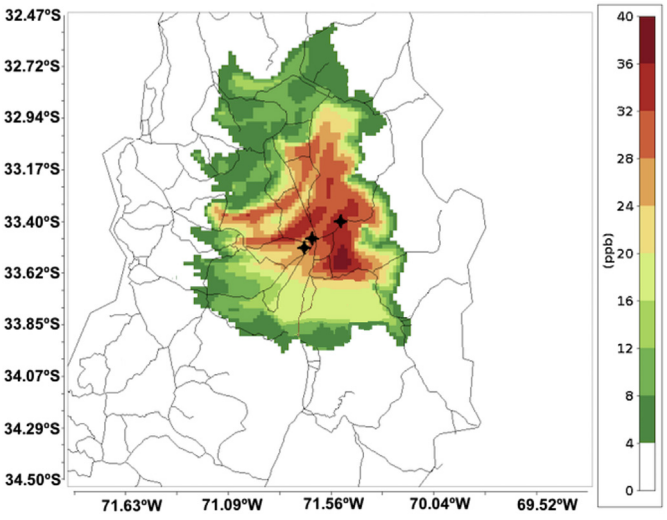

Fig. 10. Spatial distribution of ΔO_3 (i.e. O_3 mixing ratios simulated without fire emission and the highest factor applied to FINNv1 estimations, FIRE_8X) in the domain d03 for 18 LT on January 04, 2014. The stars indicate the location of the three ground stations inside Santiago.

photochemically. For the wildfire day, NO_2/NO ratios of up to 35 were reported, which is 10 times higher than the background reference of 3.5 (see Rubio et al. (2015) for an in-depth discussion of the NO/NO_2 ratios in the biomass burning plume). Fig. 11 shows the comparison between simulated and observed NO_2/NO ratios for the three analyzed stations. There is an underestimation of NO_2/NO ratios for both CER and POH stations. Although there is a noticeable increase in the observation of both NO_2 and NO, there was no major difference in the mixing ratios of these compounds calculated by WRF/Chem with and without the biomass burning emission, so there was also no difference in NO_2/NO ratios. This result suggests that there was not enough NO_2 transported in the plume to impact the relatively high urban NO_x mixing rations, and it can be related to an underestimation of NO and/or NO_2 in the FINNv1 inventory. It is important to note that during wildfires, both the combustion efficiency and the fuel nitrogen content dictate the overall NO_x emission, NO_x is emitted primarily as NO due to the combustion, which is rapidly converted to NO_2. The combustion efficiency is a measurement of how well the burnt vegetation is being utilized in the combustion process, and the fuel nitrogen content is the amount of nitrogen that can be released during the burning processes. Both factors depend on the type of vegetation, and the nitrogen content varies considerably ranging 0.2–4% (Lobert et al. 1990; Goode et al., 1999; McMeeking et al., 2009). Furthermore, the deposition of anthropogenic pollutants can enrich the nitrogen content in wildfire fuel near urban areas (Yokelson et al., 2007). Thus, the estimation of NO_x emissions and consequently the proper calculation of O_3 production become very challenging. For this reason, further verification of the area burnt (the number of fire spots compared to the number of thermal anomalies detected by MODIS, vegetation burnt compared to the vegetation classification in the model, plume height injections, etc) and improved validation of the FINNv1 fire emission estimations against observational data is needed.

4. Conclusions

In this study, a wildfire event in Santiago de Chile during the summer of 2014 has been investigated using a forward plume-rise and a chemistry (WRF/Chem) simulation. These data sets provide an opportunity to validate a regional air-quality simulation over Santiago, and a unique case to assess the performance of biomass burning plume modeling in complex topography and validated against an established air quality network. The results from the WRF/Chem model provides insights about the transport of biomass-burning plumes from the Melipilla region towards the metropolitan region of Santiago de Chile. We studied a seven-day period between January 01–07, 2014, and the impact of biomass burning plume emissions estimated by Fire Inventory from NCAR version 1 (FINNv1) on the air quality of Santiago de Chile, with a focus on day 4 (highest O_3 episode).

In a first step, we made an evaluation of some meteorological variables using observational data from three urban stations with different characteristics located inside the city of Santiago. Despite the high complexity of the region the model calculates reasonably well wind speed, wind direction, air temperature, and relative humidity. The model also provides fairly good results for vertical profiles of wind speed, wind direction, air temperature, and relative humidity.

In a second step, we first inspected the transport of an inert tracer released exactly in the locations of Melipilla region where the wildfires were captured by MODIS. While the biomass burning plume was well represented by the model, the arrival of the fire plume in Santiago was two hours later than observed in the ceilometer data. Secondly, the first three simulation days were used as a validation for the air quality simulation using RETRO global emission sources with adjustments made by Alonso et al. (2010) for Santiago de Chile region. The statistical analysis showed that the model satisfactory agreed with observations and proved to be a promising tool for air quality studies over this region. However, for the last three simulation days (during and after the wildfire event) the statistical indices showed a decrease in the model performance likely due to misrepresentation of emission sources during those

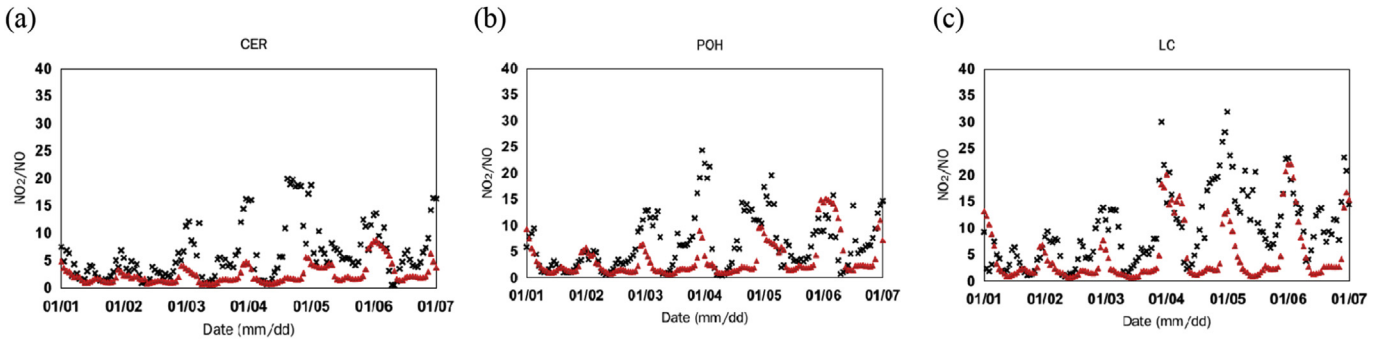

Fig. 11. Time series of the observed (crosses) and simulated (FIRE - triangles) NO_2/NO ratios for CERR (a), POH (b), LC (c), for January 1–7, 2014.

days, such as fire emissions.

In summary, this experiment showed that the more complex the case study is (in our case a combination of meteorology, chemistry, and biomass burning plume study) the less ability the model shows to capture important details of the event such as concentration, timing, and dispersion of the fire emission. As the meteorological simulation showed a good agreement with observations over a complex terrain, the air quality simulation showed a very satisfactory capability to calculate photochemical processes such O_3 formation over an urban area during days without biomass-burning events. However, when biomass burning emission were merged into the same urban atmosphere, the air quality model tends to decrease its performance. The WRF/Chem model with FINNv1 fire emission estimations presented so many uncertainties (concentrations, timing and dispersion of the fire emissions) that while the model showed a satisfactory evidence that wildfires plumes that originated in the Melipilla region were transported towards the Santiago urban area and impacted the air quality, the model still underpredicted some pollutants substantially. As stated by Wiedinmyer et al. (2011), the land use/land cover classifications and its characteristics, such as type and density of vegetation assigned to the region, where the fire spots are detected can lead to uncertainty in the emission estimations. Although the FINNv1 is a valuable tool to estimate emissions from fire, the methodology used to create this tool were based on their consistency with MODIS fire detections; so, the emission estimates were highly impacted by the variability of the ecosystem type during the study. Based on a sensitivity analysis, Wiedinmyer et al. (2011) showed that NO_x estimations can change by as much as 24% depending on the land cover input. The land coverage in the Melipilla wildfrie area was characterized by a mixture of pasture, open woodland and shrubland, including *Eucalyptus* and *Acacia caven trees* (Armesto et al., 2007; Schulz et al., 2010; Rubio et al., 2015); especially for shrubland Wiedinmyer et al. (2011) stated some high regional variation. These uncertainties in NO_x estimations can lead to major impacts in atmospheric chemistry, consequently preventing a better simulation of O_3. Thus, the Santiago case presented in this work proved to be a unique testbed for the emission inventory as it has an established air quality network, which is not necessarily available in areas with frequent biomass burning (e.g. Amazon basin, Russian taiga, biomass burning in Southeast Asia, etc.). In addition, several other factors may also explain the underestimation of calculated O_3 mixing ratios, including the lack of sufficiently temporally resolved satellite observations, the knowledge of different stages of the fire, and a robust information about emissions from the specific vegetation burnt. Additional research is needed to determine whether more observational data of fire characteristics used as input for model simulation would result in a better performance of the model.

Acknowledgments

We wish to thank the National Center for Atmospheric Research (NCAR) for valuable information provided to use FINNv1 in WRF/Chem model. Maria A. Rubio thanks DICYT—USACH 021541RC and CEDENNA-USACH. Rene Garreaud was partially supported by FONDAP Grant 15110009.

Appendix A. Supplementary data

Supplementary data related to this article can be found at http://dx.doi.org/10.1016/j.atmosenv.2017.07.002.

References

Akagi, S.K., Yokelson, R.J., Wiedinmyer, C., Alvarado, M.J., Reid, J.S., Karl, T., Crounse, J.D., Wennberg, P.O., 2011. Emission factors for open and domestic biomass burning for use in atmospheric models. Atmos. Chem. Phys. 11, 4039–4072. http://dx.doi.org/10.5194/acp-11-4039-2011.

Akagi, S.K., Yokelson, R.J., Burling, I.R., Meinardi, S., Simpson, I., Blake, D.R., McMeeking, G.R., Sullivan, A., Lee, T., Kreidenweis, S., Urbanski, S., Reardon, J., Griffith, D.W.T., Johnson, T.J., Weise, D.R., 2013. Measurements of reactive trace gases and variable O_3 formation rates in some South Carolina biomass burning plumes. Atmos. Chem. Phys. 13, 1141–1165. http://dx.doi.org/10.5194/acp-13-1141-2013.

Alonso, M.F., Longo, K.M., Freitas, S.R., Mello da Fonseca, R., Marécal, V., Pirre, M., Klenner, L.G., 2010. An urban emissions inventory for South America and its application in numerical modeling of atmospheric chemical composition at local and regional scales. Atmos. Environ. 44, 5072–5083. http://dx.doi.org/10.1016/j.atmosenv.2010.09.013.

Alvarado, M.J., Prinn, R.G., 2009. Formation of ozone and growth of aerosols in young smoke plumes from biomass burning: 1. Lagrangian parcel studies. J. Geophys. Res. 114, D09306. http://dx.doi.org/10.1029/2008JD011144.

Alvarado, M.J., Logan, J.A., Mao, J., Apel, E., Riemer, D., Blake, D., Cohen, R.C., Min, K.-E., Perring, A.E., Browne, E.C., Wooldridge, P.J., Diskin, G.S., Sachse, G.W., Fuelberg, H., Sessions, W.R., Harrigan, D.L., Huey, G., Liao, J., Case-Hanks, A., Jimenez, J.L., Cubison, M.J., Vay, S.A., Weinheimer, A.J., Knapp, D.J., Montzka, D.D., Flocke, F.M., Pollack, I.B., Wennberg, P.O., Kurten, A., Crounse, J., Clair, J.M.S., Wisthaler, A., Mikoviny, T., Yantosca, R.M., Carouge, C.C., Le Sager, P., 2010. Nitrogen oxides and PAN in plumes from boreal fires during ARCTAS-B and their impact on ozone: an integrated analysis of aircraft and satellite observations. Atmos. Chem. Phys. 10, 9739–9760. http://dx.doi.org/10.5194/acp-10-9739-2010.

Armesto, J., Arroyo, M.T.K., Hinojosa, L.F., 2007. The Mediterranean environment of central Chile. In: Veblen, T., Young, K., Orme, A. (Eds.), The Physical Geography of South America. Oxford University Press, Oxford, UK.

Bertschi, I.T., Jaffe, D.A., 2005. Long-range transport of ozone, carbon monoxide, and aerosols to the NE Pacific troposphere during the summer of 2003: observations of smoke plumes from Asian boreal fires. J. Geophys. Res. 110, D05303. http://dx.doi.org/10.1029/2004JD005135.

Bond, T.C., Streets, D.G., Yarber, K.F., Nelson, S.M., Woo, J.-H., Klimont, Z., 2004. A technology-based global inventory of black and organic carbon emissions from combustion. J. Geophys. Res. 109, D14203. http://dx.doi.org/10.1029/2003JD003697.

Chalbot, M.-C., Kavouras, L.G., Dubois, D.W., 2013. Assessment of the Contribution of Wildfires to Ozone Concentrations in the Central US-Mexico Border Region. Aerosol and Air Quality Research. http://dx.doi.org/10.4209/aaqr.2012.08.0232.

Chatfield, R.B., Vastano, J.A., Singh, H.B., Sachse, G., 1996. A general model of how fire emissions and chemistry produce African/oceanic plumes (O_3, CO, PAN, smoke) in TRACE A. J. Geophys. Res. 101, 24279–24306. http://dx.doi.org/10.1029/96JD01871.

Cheng, L., McDonald, K.M., Angle, R.P., Sandhu, H.S., 1998. Forest fire enhanced photochemical air pollution. A case study. Atmos. Environ. 32, 673–681. http://dx.doi.org/10.1016/S1352-2310(97)00319-1.

Colarco, P.R., Schoeberl, M.R., Doddridge, B.G., Marufu, L.T., Torres, O., Welton, E.J., 2004. Transport of smoke from Canadian forest fires to the surface near Washington, D.C.: injection height, entrainment, and optical properties. J. Geophys. Res. 109, D06203. http://dx.doi.org/10.1029/2003JD004248.

Cook, P.A., Savage, N.H., Turquety, S., Carver, G.D., O'Connor, F.M., Heckel, A., Stewart, D., Whalley, L.K., Parker, A.E., Schlager, H., Singh, H.B., Avery, M.A., Sachse, G.W., Brune, W., Richter, A., Burrows, J.P., Purvis, R., Lewis, A.C., Reeves, C.E., Monks, P.S., Levine, J.G., Pyle, J.A., 2007. Forest fire plumes over the North Atlantic: p-TOMCAT model simulations with aircraft and satellite measurements from the ITOP/ICARTT campaign. J. Geophys. Res. 112, D10S43. http://dx.doi.org/10.1029/2006JD007563.

Crutzen, P.J., Andreae, M.O., 1990. Biomass burning in the tropics: impact on atmospheric chemistry and biogeochemical cycles. Science 250, 1669–1678. http://dx.doi.org/10.1126/science.250.4988.1669.

Czader, B.H., Li, X., Rappenglück, B., 2013. CMAQ modeling and analysis of radicals, radical precursors and chemical transformations. J. Geophys. Res. 118, 11,376–11,387. http://dx.doi.org/10.1002/jgrd.50807.

Delany, A.C., Haagensen, P., Walters, S., Wartburg, A.F., Crutzen, P.J., 1985. Photochemically produced ozone in the emission from large-scale tropical vegetation fires. J. Geophys. Res. 90, 2425–2429. http://dx.doi.org/10.1029/JD090iD01p02425.

Elshorbany, Y.F., Kleffmann, J., Kurtenbach, R., Lissi, E., Rubio, M.A., Villena, G., Gramsch, E., Rickard, A.R., Pilling, M.J., Wiesen, P., 2009. Summertime photochemical ozone formation in Santiago, Chile. Atmos. Environ. 43, 6398–6407.

Emmons, L.K., Walters, S., Hess, P.G., Lamarque, J.-F., Pfister, G.G., Fillmore, D., Granier, C., Guenther, A., Kinnison, D., Laepple, T., Orlando, J., Tie, X., Tyndall, G., Wiedinmyer, C., Baughcum, S.L., Kloster, S., 2010. Description and evaluation of the model for ozone and related chemical tracers, version 4 (MOZART-4). Geosci. Model Dev. 3, 43–67. http://dx.doi.org/10.5194/gmd-3-43-2010.

Evans, L.F., King, N.K., Packham, D.R., Stephens, E.T., 1974. Ozone measurements in smoke from forest fires. Environ. Sci. Technol. 8, 75–76. http://dx.doi.org/10.1021/es60086a013.

Fishman, J., Watson, C.E., Larsen, J.C., Logan, J.A., 1990. Distribution of tropospheric

ozone determined from satellite data. J. Geophys. Res. 95, 3599–3617. http://dx.doi.org/10.1029/JD095iD04p03599.
Forster, C., Wandinger, U., Wotawa, G., James, P., Mattis, I., Althausen, D., Simmonds, P., O'Doherty, S., Jennings, S.G., Kleefeld, C., Schneider, J., Trickl, T., Kreipl, S., Jäger, H., Stohl, A., 2001. Transport of boreal forest fire emissions from Canada to Europe. J. Geophys. Res. 106, 22887–22906. http://dx.doi.org/10.1029/2001JD900115.
Freitas, S.R., Longo, K.M., Alonso, M.F., Pirre, M., Marecal, V., Grell, G., Stockler, R., Mello, R.F., Sánchez Gácita, M., 2011. PREP-CHEM-SRC – 1.0: a preprocessor of trace gas and aerosol emission fields for regional and global atmospheric chemistry models. Geosci. Model Dev. 4, 419–433. http://dx.doi.org/10.5194/gmd-4-419-2011.
Fujiwara, M., Kita, K., Kawakami, S., Ogawa, T., Komala, N., Saraspriya, S., Suripto, A., 1999. Tropospheric ozone enhancements during the Indonesian Forest Fire Events in 1994 and in 1997 as revealed by ground-based observations. Geophys. Res. Lett. 26, 2417–2420. http://dx.doi.org/10.1029/1999GL900117.
Galanter, M., Levy, H., Carmichael, G.R., 2000. Impacts of biomass burning on tropospheric CO, NO_x, and O_3. J. Geophys. Res. 105, 6633–6653. http://dx.doi.org/10.1029/1999JD901113.
Gallardo, K., 2014. Así se ve el incendio forestal de Melipilla desde las alturas [WWW Document], 24horas.cl. http://www.24horas.cl/nacional/asi-se-ve-el-incendio-forestal-de-melipilla-desde-las-alturas-1012198 (Accessed 6 January 2017).
Giglio, L., van der Werf, G.R., Randerson, J.T., Collatz, G.J., Kasibhatla, P., 2006. Global estimation of burned area using MODIS active fire observations. Atmos. Chem. Phys. 6, 957–974. http://dx.doi.org/10.5194/acp-6-957-2006.
Goode, J.G., Yokelson, R.J., Susott, R.A., Ward, D.E., 1999. Trace gas emissions from laboratory biomass fires measured by open-path Fourier transform infrared spectroscopy: fires in grass and surface fuels. J. Geophys. Res. 104, 21237–21245. http://dx.doi.org/10.1029/1999JD900360.
Grell, G.A., Freitas, S.R., 2014. A scale and aerosol aware stochastic convective parameterization for weather and air quality modeling. Atmos. Chem. Phys. 14, 5233–5250. http://dx.doi.org/10.5194/acp-14-5233-2014.
Grell, G.A., Peckham, S.E., Schmitz, R., McKeen, S.A., Frost, G., Skamarock, W.C., Eder, B., 2005. Fully coupled "online" chemistry within the WRF model. Atmos. Environ. 39, 6957–6975. http://dx.doi.org/10.1016/j.atmosenv.2005.04.027.
Guenther, A., Karl, T., Harley, P., Wiedinmyer, C., Palmer, P.I., Geron, C., 2006. Estimates of global terrestrial isoprene emissions using MEGAN (model of emissions of gases and aerosols from nature). Atmos. Chem. Phys. 6, 3181–3210. http://dx.doi.org/10.5194/acp-6-3181-2006.
Hauglustaine, D.A., Brasseur, G.P., Levine, J.S., 1999. A sensitivity simulation of tropospheric ozone changes due to the 1997 Indonesian fire emissions. Geophys. Res. Lett. 26, 3305–3308. http://dx.doi.org/10.1029/1999GL900610.
Hong, S.-Y., Noh, Y., Dudhia, J., 2006. A new vertical diffusion package with an explicit treatment of entrainment processes. Mon. Wea. Rev. 134, 2318–2341. http://dx.doi.org/10.1175/MWR3199.1.
IPCC, 2007. Climate Change 2007 – Synthesis Report.
Jaffe, D.A., Wigder, N.L., 2012. Ozone production from wildfires: a critical review. Atmos. Environ. 51, 1–10. http://dx.doi.org/10.1016/j.atmosenv.2011.11.063.
Jaffe, D., Anderson, T., Covert, D., Trost, B., Danielson, J., Simpson, W., Blake, D., Harris, J., Streets, D., 2001. Observations of ozone and related species in the northeast Pacific during the PHOBEA campaigns: 1. Ground-based observations at Cheeka Peak. J. Geophys. Res. 106, 7449–7461. http://dx.doi.org/10.1029/2000JD900636.
Jaffe, D., Bertschi, I., Jaeglé, L., Novelli, P., Reid, J.S., Tanimoto, H., Vingarzan, R., Westphal, D.L., 2004. Long-range transport of Siberian biomass burning emissions and impact on surface ozone in western North America. Geophys. Res. Lett. 31, L16106. http://dx.doi.org/10.1029/2004GL020093.
Junquera, V., Russell, M.M., Vizuete, W., Kimura, Y., Allen, D., 2005. Wildfires in eastern Texas in August and September 2000: Emissions, aircraft measurements, and impact on photochemistry. Atmos. Environ. 39, 4983–4996. http://dx.doi.org/10.1016/j.atmosenv.2005.05.004.
Kaufman, Y.J., Setzer, A., Ward, D., Tanre, D., Holben, B.N., Menzel, P., Pereira, M.C., Rasmussen, R., 1992. Biomass burning airborne and spaceborne experiment in the amazonas (BASE-A). J. Geophys. Res. 97, 14581–14599. http://dx.doi.org/10.1029/92JD00275.
Kita, K., Fujiwara, M., Kawakami, S., 2000. Total ozone increase associated with forest fires over the Indonesian region and its relation to the El Niño-Southern oscillation. Atmos. Environ. 34, 2681–2690. http://dx.doi.org/10.1016/S1352-2310(99)00522-1.
Kondo, Y., Morino, Y., Takegawa, N., Koike, M., Kita, K., Miyazaki, Y., Sachse, G.W., Vay, S.A., Avery, M.A., Flocke, F., Weinheimer, A.J., Eisele, F.L., Zondlo, M.A., Weber, R.J., Singh, H.B., Chen, G., Crawford, J., Blake, D.R., Fuelberg, H.E., Clarke, A.D., Talbot, R.W., Sandholm, S.T., Browell, E.V., Streets, D.G., Liley, B., 2004. Impacts of biomass burning in Southeast Asia on ozone and reactive nitrogen over the western Pacific in spring. J. Geophys. Res. 109, D15S12. http://dx.doi.org/10.1029/2003JD004203.
Lapina, K., Honrath, R.E., Owen, R.C., Val Martín, M., Pfister, G., 2006. Evidence of significant large-scale impacts of boreal fires on ozone levels in the midlatitude Northern Hemisphere free troposphere. Geophys. Res. Lett. 33, L10815. http://dx.doi.org/10.1029/2006GL025878.
Lei, W., Li, G., Molina, L.T., 2013. Modeling the impacts of biomass burning on air quality in and around Mexico City. Atmos. Chem. Phys. 13, 2299–2319. http://dx.doi.org/10.5194/acp-13-2299-2013.
Leung, F.-Y.T., Logan, J.A., Park, R., Hyer, E., Kasischke, E., Streets, D., Yurganov, L., 2007. Impacts of enhanced biomass burning in the boreal forests in 1998 on tropospheric chemistry and the sensitivity of model results to the injection height of emissions. J. Geophys. Res. 112, D10313. http://dx.doi.org/10.1029/2006JD008132.
Lin, Y.-L., Farley, R.D., Orville, H.D., 1983. Bulk parameterization of the snow field in a cloud model. J. Clim. Appl. Meteor 22, 1065–1092. http://dx.doi.org/10.1175/1520-0450(1983)022<1065:BPOTSF>2.0.CO;2.
Liu, H., Jacob, D.J., Chan, L.Y., Oltmans, S.J., Bey, I., Yantosca, R.M., Harris, J.M., Duncan, B.N., Martin, R.V., 2002. Sources of tropospheric ozone along the Asian Pacific Rim: an analysis of ozonesonde observations. J. Geophys. Res. 107, 4573. http://dx.doi.org/10.1029/2001JD002005.
Lobert, J.M., Scharffe, D.H., Hao, W.M., Crutzen, P.J., 1990. Importance of biomass burning in the atmospheric budgets of nitrogen-containing gases. Nature 346, 552–554. http://dx.doi.org/10.1038/346552a0.
Martins, V., Miranda, A.I., Carvalho, A., Schaap, M., Borrego, C., Sá, E., 2012. Impact of forest fires on particulate matter and ozone levels during the 2003, 2004 and 2005 fire seasons in Portugal. Sci. Total Environ. 414, 53–62. http://dx.doi.org/10.1016/j.scitotenv.2011.10.007.
Mason, S.A., Trentmann, J., Winterrath, T., Yokelson, R.J., Christian, T.J., Carlson, L.J., Warner, T.R., Wolfe, L.C., Andreae, M.O., 2006. Intercomparison of two box models of the chemical evolution in biomass-burning smoke plumes. J. Atmos. Chem. 55, 273–297. http://dx.doi.org/10.1007/s10874-006-9039-5.
McKeen, S.A., Wotawa, G., Parrish, D.D., Holloway, J.S., Buhr, M.P., Hübler, G., Fehsenfeld, F.C., Meagher, J.F., 2002. Ozone production from Canadian wildfires during June and july of 1995. J. Geophys. Res. 107 http://dx.doi.org/10.1029/2001JD000697. ACH 7–1.
McMeeking, G.R., Kreidenweis, S.M., Baker, S., Carrico, C.M., Chow, J.C., Collett, J.L., Hao, W.M., Holden, A.S., Kirchstetter, T.W., Malm, W.C., Moosmüller, H., Sullivan, A.P., Wold, C.E., 2009. Emissions of trace gases and aerosols during the open combustion of biomass in the laboratory. J. Geophys. Res. 114, D19210. http://dx.doi.org/10.1029/2009JD011836.
Mlawer, E.J., Taubman, S.J., Brown, P.D., Iacono, M.J., Clough, S.A., 1997. Radiative transfer for inhomogeneous atmospheres: RRTM, a validated correlated-k model for the longwave. J. Geophys. Res. 102, 16663–16682. http://dx.doi.org/10.1029/97JD00237.
Morris, G.A., Hersey, S., Thompson, A.M., Pawson, S., Nielsen, J.E., Colarco, P.R., McMillan, W.W., Stohl, A., Turquety, S., Warner, J., Johnson, B.J., Kucsera, T.L., Larko, D.E., Oltmans, S.J., Witte, J.C., 2006. Alaskan and Canadian forest fires exacerbate ozone pollution over Houston, Texas, on 19 and 20 July 2004. J. Geophys. Res. 111, D24S03. http://dx.doi.org/10.1029/2006JD007090.
Nassar, R., Logan, J.A., Megretskaia, I.A., Murray, L.T., Zhang, L., Jones, D.B.A., 2009. Analysis of tropical tropospheric ozone, carbon monoxide, and water vapor during the 2006 El Niño using TES observations and the GEOS-Chem model. J. Geophys. Res. 114, D17304. http://dx.doi.org/10.1029/2009JD011760.
Oltmans, S.J., Lefohn, A.S., Harris, J.M., Tarasick, D.W., Thompson, A.M., Wernli, H., Johnson, B.J., Novelli, P.C., Montzka, S.A., Ray, J.D., Patrick, L.C., Sweeney, C., Jefferson, A., Dann, T., Davies, J., Shapiro, M., Holben, B.N., 2010. Enhanced ozone over western North America from biomass burning in Eurasia during April 2008 as seen in surface and profile observations. Atmos. Environ. 44, 4497–4509. http://dx.doi.org/10.1016/j.atmosenv.2010.07.004.
Pfister, G.G., Emmons, L.K., Hess, P.G., Honrath, R., Lamarque, J.-F., Val Martin, M., Owen, R.C., Avery, M.A., Browell, E.V., Holloway, J.S., Nedelec, P., Purvis, R., Ryerson, T.B., Sachse, G.W., Schlager, H., 2006. Ozone production from the 2004 North American boreal fires. J. Geophys. Res. 111, D24S07. http://dx.doi.org/10.1029/2006JD007695.
Pfister, G.G., Wiedinmyer, C., Emmons, L.K., 2008. Impacts of the fall 2007 California wildfires on surface ozone: integrating local observations with global model simulations. Geophys. Res. Lett. 35, L19814. http://dx.doi.org/10.1029/2008GL034747.
Pfister, G.G., Parrish, D.D., Worden, H., Emmons, L.K., Edwards, D.P., Wiedinmyer, C., Diskin, G.S., Huey, G., Oltmans, S.J., Thouret, V., Weinheimer, A., Wisthaler, A., 2011. Characterizing summertime chemical boundary conditions for airmasses entering the US West Coast. Atmos. Chem. Phys. 11, 1769–1790. http://dx.doi.org/10.5194/acp-11-1769-2011.
Phadnis, M.J., Carmichael, G.R., 2000. Forest fire in the Boreal Region of China and its impact on the photochemical oxidant cycle of East Asia. Atmos. Environ. 34, 483–498. http://dx.doi.org/10.1016/S1352-2310(99)00249-6.
Randerson, J.T., van der Werf, G.R., Giglio, L., Collatz, G.J., Kasibhatla, P.S., 2015. Global Fire Emissions Database, Version 4, (GFEDv4). ORNL DAAC, Oak Ridge, Tennessee, USA. https://doi.org/10.3334/ORNLDAAC/1293.
Rappenglück, B., Oyola, P., Olaeta, I., Fabian, P., 2000. The evolution of photochemical smog in the Metropolitan Area of Santiago de Chile. J. Appl. Meteor. 39, 275–290.
Rappenglück, B., Schmitz, R., Bauerfeind, M., Cereceda-Balic, F., v. Baer, D., Jorquera, H., Silva, Y., Oyola, P., 2005. An urban photochemistry study in Santiago de Chile. Atmos. Environ. 39, 2913–2931. http://dx.doi.org/10.1016/j.atmosenv .2004.12.049.
Real, E., Law, K.S., Weinzierl, B., Fiebig, M., Petzold, A., Wild, O., Methven, J., Arnold, S., Stohl, A., Huntrieser, H., Roiger, A., Schlager, H., Stewart, D., Avery, M., Sachse, G., Browell, E., Ferrare, R., Blake, D., 2007. Processes influencing ozone levels in Alaskan forest fire plumes during long-range transport over the North Atlantic. J. Geophys. Res. 112, D10S41. http://dx.doi.org/10.1029/2006JD007576.
Reid, J.S., Hyer, E.J., Prins, E.M., Westphal, D.L., Zhang, J., Wang, J., Christopher, S.A., Curtis, C.A., Schmidt, C.C., Eleuterio, D.P., Richardson, K.A., Hoffman, J.P., 2009. Global monitoring and forecasting of biomass-burning smoke: description of

and lessons from the fire locating and modeling of burning emissions (FLAMBE) program. IEEE J. Sel. Top. Appl. Earth Obs. Remote Sens. 2 (3), 144–162. http://dx.doi.org/10.1109/jstars.2009.2027443.

Rubio, M.A., Lissi, E., Gramsch, E., Garreaud, R.D., 2015. Effect of nearby forest fires on ground level ozone concentrations in Santiago, Chile. Atmosphere 6, 1926–1938. http://dx.doi.org/10.3390/atmos6121838.

Rutllant, J., Garreaud, R., 2004. Episodes of strong flow down the western slope of the subtropical Andes. Mon. Wea. Rev. 132, 611–622. http://dx.doi.org/10.1175/1520-0493.

Schulz, J.J., Cayuela, L., Echeverria, C., Salas, J., Rey Benayas, J.M., 2010. Monitoring land cover change of the dryland forest landscape of Central Chile (1975–2008). Appl. Geogr. 30, 436–447. http://dx.doi.org/10.1016/j.apgeog.2009.12.003.

Seinfeld, J.S., Pandis, S.N., 2016. Atmospheric Chemistry and Physics: From Air Pollution to Climate Change, 3rd Edition. New York.

Singh, H.B., Anderson, B.E., Brune, W.H., Cai, C., Cohen, R.C., Crawford, J.H., Cubison, M.J., Czech, E.P., Emmons, L., Fuelberg, H.E., Huey, G., Jacob, D.J., Jimenez, J.L., Kaduwela, A., Kondo, Y., Mao, J., Olson, J.R., Sachse, G.W., Vay, S.A., Weinheimer, A., Wennberg, P.O., Wisthaler, A., 2010. Pollution influences on atmospheric composition and chemistry at high northern latitudes: boreal and California forest fire emissions. Atmos. Environ. 44, 4553–4564. http://dx.doi.org/10.1016/j.atmosenv.2010.08.026.

Sinha, P., Jaeglé, L., Hobbs, P.V., Liang, Q., 2004. Transport of biomass burning emissions from southern Africa. J. Geophys. Res. 109, D20204. http://dx.doi.org/10.1029/2004JD005044.

Stith, J.L., Radke, L.F., Hobbs, P.V., 1981. Particle emissions and the production of ozone and nitrogen oxides from the burning of forest slash. Atmos. Environ. 15, 73–82. http://dx.doi.org/10.1016/0004-6981(81)90127-X, 1967.

Stockwell, W.R., Kirchner, F., Kuhn, M., Seefeld, S., 1997. A new mechanism for regional atmospheric chemistry modeling. J. Geophys. Res. 102, 25847–25879. http://dx.doi.org/10.1029/97JD00849.

Tewari, M., Chen, F., Wang, W., Dudhia, J., LeMone, M.A., Mitchell, K., Ek, M., Gayno, G., Wegiel, J., Cuenca, R.H., 2004. Implementation and verification of the unified NOAH land surface model in the WRF model. In: 20th Conference on Weather Analysis and Forecasting/16th Conference on Numerical Weather Prediction, pp. 11–15.

Thompson, A.M., Pickering, K.E., McNamara, D.P., Schoeberl, M.R., Hudson, R.D., Kim, J.H., Browell, E.V., Kirchhoff, V.W.J.H., Nganga, D., 1996. Where did tropospheric ozone over southern Africa and the tropical Atlantic come from in October 1992? Insights from TOMS, GTE TRACE A, and SAFARI 1992. J. Geophys. Res. 101, 24251–24278. http://dx.doi.org/10.1029/96JD01463.

Thompson, A.M., Witte, J.C., Hudson, R.D., Guo, H., Herman, J.R., Fujiwara, M., 2001. Tropical tropospheric ozone and biomass burning. Science 291, 2128–2132. http://dx.doi.org/10.1126/science.291.5511.2128.

Trentmann, J., Andreae, M.O., Graf, H.-F., 2003. Chemical processes in a young biomass-burning plume. J. Geophys. Res. 108, 4705. http://dx.doi.org/10.1029/2003JD003732.

Trentmann, J., Yokelson, R.J., Hobbs, P.V., Winterrath, T., Christian, T.J., Andreae, M.O., Mason, S.A., 2005. An analysis of the chemical processes in the smoke plume from a savanna fire. J. Geophys. Res. 110, D12301. http://dx.doi.org/10.1029/2004JD005628.

Val Martín, M., Honrath, R.E., Owen, R.C., Pfister, G., Fialho, P., Barata, F., 2006. Significant enhancements of nitrogen oxides, black carbon, and ozone in the North Atlantic lower free troposphere resulting from North American boreal wildfires. J. Geophys. Res. 111, D23S60. http://dx.doi.org/10.1029/2006JD007530.

Val Martín, M., Honrath, R.E., Owen, R.C., Lapina, K., 2008. Large-scale impacts of anthropogenic pollution and boreal wildfires on the nitrogen oxides over the central North Atlantic region. J. Geophys. Res. 113, D17308. http://dx.doi.org/10.1029/2007JD009689.

Wiedinmyer, C., Quayle, B., Geron, C., Belote, A., McKenzie, D., Zhang, X., O'Neill, S., Wynne, K.K., 2006. Estimating emissions from fires in North America for air quality modeling. Atmos. Environ. 40, 3419–3432. http://dx.doi.org/10.1016/j.atmosenv.2006.02.010.

Wiedinmyer, C., Akagi, S.K., Yokelson, R.J., Emmons, L.K., Al-Saadi, J.A., Orlando, J.J., Soja, A.J., 2011. The Fire INventory from NCAR (FINN): a high resolution global model to estimate the emissions from open burning. Geosci. Model Dev. 4, 625–641. http://dx.doi.org/10.5194/gmd-4-625-2011.

Yokelson, R.J., Bertschi, I.T., Christian, T.J., Hobbs, P.V., Ward, D.E., Hao, W.M., 2003. Trace gas measurements in nascent, aged, and cloud-processed smoke from African savanna fires by airborne Fourier transform infrared spectroscopy (AFTIR). J. Geophys. Res. 108, 8478. http://dx.doi.org/10.1029/2002JD002322.

Yokelson, R.J., Urbanski, S.P., Atlas, E.L., Toohey, D.W., Alvarado, E.C., Crounse, J.D., Wennberg, P.O., Fisher, M.E., Wold, C.E., Campos, T.L., Adachi, K., Buseck, P.R., Hao, W.M., 2007. Emissions from forest fires near Mexico City. Atmos. Chem. Phys. 7, 5569–5584. http://dx.doi.org/10.5194/acp-7-5569-2007.

Yokelson, R.J., Crounse, J.D., DeCarlo, P.F., Karl, T., Urbanski, S., Atlas, E., Campos, T., Shinozuka, Y., Kapustin, V., Clarke, A.D., Weinheimer, A., Knapp, D.J., Montzka, D.D., Holloway, J., Weibring, P., Flocke, F., Zheng, W., Toohey, D., Wennberg, P.O., Wiedinmyer, C., Mauldin, L., Fried, A., Richter, D., Walega, J., Jimenez, J.L., Adachi, K., Buseck, P.R., Hall, S.R., Shetter, R., 2009. Emissions from biomass burning in the Yucatan. Atmos. Chem. Phys. 9, 5785–5812. http://dx.doi.org/10.5194/acp-9-5785-2009.